Research Article | Vol. 24, No. 20 | 3 Oct 2016 | OPTICS EXPRESS 23221

Optics EXPRESS

Transverse pump-probe microscopy of moving breakdown, filamentation and self-organized absorption in alkali aluminosilicate glass using ultrashort pulse laser

DANIEL GROSSMANN,[1,2,*] MARTIN REININGHAUS,[3,2] CHRISTIAN KALUPKA,[2] MALTE KUMKAR,[1] AND REINHART POPRAWE[3,2]

[1]*TRUMPF Laser- und Systemtechnik GmbH, Johann-Maus-Strasse 2, 71254 Ditzingen, Germany*
[2]*Chair for Laser Technology, RWTH Aachen University, Steinbachstr 15, 52074 Aachen, Germany*
[3]*Fraunhofer Institute for Laser Technology ILT, Steinbachstr 15, 52074 Aachen, Germany*
[*]*daniel.grossmann@de.trumpf.com*

Abstract: We present time and space resolved transverse pump-probe measurements of the free electron and defect generation induced by nonlinear absorption of ultra short pulsed laser radiation in unhardened Corning Gorilla glass. The applied setup exhibits a 100 fs probe pulse duration and an independent pump pulse duration up to 5 ps. Hence, our work comprises the absorption of ultra short pulsed laser radiation at a wavelength of 800 nm and pulse energies from 10 μJ to 50 μJ up to a delay of 6 ns. Our investigations reveal different absorption regimes like filamentation and moving breakdown as well as the formation of permanent modifications. Finally, the deposition of multiple pulses in the incubation regime is examined, observing a self-organizing absorption effect.

OCIS codes: (100.0118) Imaging ultrafast phenomena; (320.7110) Ultrafast nonlinear optics; (190.3270) Kerr effect; (260.5950) Self-focusing; (320.7100) Ultrafast measurements; (140.3390) Laser materials processing.

References and links

1. R. R. Gattass and E. Mazur, "Femtosecond laser micromachinig in transparent materials," Nat. Photonics **2**, 219–225 (2008).
2. M. Kumkar, L. Bauer, S. Russ, M. Wendel, J. Kleiner, D. Grossmann, K. Bergner and S. Nolte, "Comparison of different processes for separation of glass and crystals using ultrashort pulsed lasers," Proc. SPIE **8972**, 897214 (2014).
3. K. Miura, J. Qiu, H. Inouye, T. Mitsuyu, and K. Hirao, "Photowritten optical waveguides in various glasses with ultrashort pulse laser," Appl. Phys. Lett. **71**, 3329 (1997).
4. W. Watanabe, S. Onda, T. Tamaki, K. Itoh, and J. Nishii, "Space-selective laser joining of dissimilar transparent materials using femtosecond laser pulses," Appl. Phys. Lett. **89**, 021106 (2006).
5. A. Marcinkevicius, S. Juodkazis, M. Watanabe, M. Miwa, S. Matsuo, H. Misawa and J. Nishii, "Femtosecond laser-assisted three-dimensional microfabrication in silica," Opt. Lett. **26**, 277–279 (2001).
6. M. Kumkar, M. Kaiser, J. Kleiner, D. Grossmann, D. Flamm, K Bergner and S. Nolte, "Cutting of Transparent Materials by Tailored Absorption," in *Advanced Solid State Lasers*, OSA Technical Digest (online) (Optical Society of America, 2014), paper ATh1A.2.
7. A. Couairon, A. Mysyrowicz, " Femtosecond filamentation in transparent media, " Physics Reports **441**, 47–189 (2007).
8. S. S. Mao, F. Quere, S. Guizard, X. Mao, R.E. Russo, G. Petite and P. Martin, "Dynamics of femtosecond laser interactions with dielectrics," Appl. Phys. A **79**, 1695–1709 (2004).
9. M. Lancry, B. Poumellec, R. Desmarchelier, and B. Bourguignon, "Oriented creation of anisotropic defects by IR femtosecond laser scanning in silica, " Opt. Mater. Express **2**, 1809–1821 (2012).
10. L. Skuja, K. Kajihara, T. Kinoshita, M. Hirano, and H. Hosono, "The behavior of interstitial oxygen atoms induced by F_2 laser irradiation of oxygen-rich glassy SiO_2," Nucl. Instrum. Methods Phys. Res. B **191**, 127–130 (2002).
11. K. Mishchik, A. Ferrer, A. Ruiz de la Cruz, A. Mermillod-Blondin, C. Mauclair, Y. Ouerdane, A. Boukenter, J. Solis, and R. Stoian, "Photoinscription domains for ultrafast laser writing of refractive index changes in BK7 borosilicate crown optical glass," Opt. Mater. Express **3**, 67–85 (2013).
12. A. Mermillod-Blondin, I. M. Burakov, Yu. P. Meshcheryakov, N. M. Bulgakova, E. Audouard, A. Rosenfeld, A. Husakou, I. V. Hertel, and R. Stoian, "Flipping the sign of refractive index changes in ultrafast and temporally shaped laser-irradiated borosilicate crown optical glass at high repetition rates," Phys. Rev. B **77**, 104205 (2008).

#272114 http://dx.doi.org/10.1364/OE.24.023221
Journal © 2016 Received 22 Jul 2016; revised 3 Sep 2016; accepted 4 Sep 2016; published 27 Sep 2016

Optics EXPRESS

13. E. G. Gamaly, S. Juodkazis, K. Nishimura, H. Misawa, B. Luther-Davies, L. Hallo, P. Nicolai, and V. T. Tikhonchuk, "Laser-matter interaction in the bulk of a transparent solid: Confined microexplosion and void formation," Phys. Rev. B **73**, 214101 (2006).
14. Q. Sun, H. Jiang, Y. Liu, Z. Wu, H. Yang, and Q. Gong, "Measurement of the collision time of dense electronic plasma induced by a femtosecond laser in fused silica," Opt. Lett. **30**, 320–322 (2005).
15. C. Shen, M. Chambonneau, X. Cheng, Z. Xu, and T. Jiang, "Identification of the formation phases of filamentary damage induced by nanosecond laser pulses in bulk fused silica," Appl. Phys. Lett. **107**, 111101 (2015).
16. D. Puerto, J. Siegel, W. Gawelda, M. Galvan-Sosa, L. Ehrentraut, J. Bonse, and J. Solis, "Dynamics of plasma formation, relaxation, and topography modification induced by femtosecond laser pulses in crystalline and amorphous dielectrics," J. Opt. Soc. Am. B **27**, 1065–1076 (2010).
17. M. Sakakura, T. Tochio, M. Eida, Y. Shimotsuma, S. Kanehira, M. Nishi, K. Miura, and K. Hirao, "Observation of laser-induced stress waves and mechanism of structural changes inside rock-salt crystals," Opt. Express **19**, 17780–17789 (2011).
18. A. Mermillod-Blondin, C. Mauclair, J. Bonse, R. Stoian, E. Audouard, A. Rosenfeld, and I.V. Hertel, 'Time-resolved imaging of laser-induced refractive index changes in transparent media," Rev. Sci. Instrum. **82**, 033703 (2011).
19. D.G. Papazoglou, and S. Tzortzakis, "In-line holography for the characterization of ultrafast laser filamentation in transparent media," Appl. Phys. Lett. **93**, 041120 (2008).
20. Y. Hayaski, K. Iwata, S. Hasegawa, A. Takita, and S. Juodkazis, "Time-resolved axial-view of the dielectric breakdown under tight focusing in glass, " Opt. Mater. Express. **1**, 1399–1408 (2011).
21. C. Mauclair, K. Mishchik, A. Mermillod-Blondin, A. Rosenfeld, I.V. Hertel, E. Audouard, and R. Stoian., "Optimization of the energy deposition in glasses with temporally-shaped femtosecond laser pulses," Phys. Procedia **12**, 76–81 (2011).
22. D. X. Hammer, E. D. Jansen, M. Frenz, G. D. Noojin, R. J. Thomas, J. Noack, A. Vogel, B. A. Rockwell, and A. J Welch, "Shielding properties of laser-induced breakdown in water for pulse durations from 5 ns to 125 fs," Appl. Opt. **36**, 5630–5640 (1997).
23. G. Fibich and A. L. Gaeta, "Critical power for self-focusing in bulk media and in hollow waveguides," Opt. Lett. **25**, 335–337 (2000).
24. U. Loeschner, S. Mauersberger, R. Ebert, H. Exner, J. Schille, P. Regenfuss and L. Hartwig, "Micromachining of glass with short ns-pulses and highly repetitive fs-laser pulses," Proc. ICALEO **403**, 193–201 (2008).
25. M. Grehn, T. Seuthe, W. Tsai, M. Hoefner, A. Achtstein, A. Mermillod-Blondin, M. Eberstein, H. Eichler, and J. Bonse, "Nonlinear absorption and refraction of binary and ternary alkaline and alkaline earth silicate glasses," Opt. Mater. Express **3**, 2132–2140 (2013).
26. W. Gawelda, D. Puerto, J. Siegel, A. Ferrer, A. Ruiz de la Cruz, H. FernÃąndez, and J. Solis, "Ultrafast imaging of transient electronic plasmas produced in conditions of femtosecond waveguide writing in dielectrics," Appl. Phys. Lett. **93**, 121109 (2008).
27. N. T. Nguyen, A. Saliminia, W. Liu, S. L. Chin, and R. Vallee, "Optical breakdown versus filamentation in fused silica by use of femtosecond infrared laser pulses," Opt. Lett. **28**, 1591–1593 (2003).
28. J. B. Ashcom, R. R. Gattass, C. B. Schaffer, and E. Mazur, "Numerical aperture dependence of damage and supercontinuum generation from femtosecond laser pulses in bulk fused silica," J. Opt. Soc. Am. B **23**, 2317–2322 (2006).
29. E. Gaizauskas, E. Vanagas, V. Jarutis, S. Juodkazis, V. Mizeikis, and H. Misawa, "Discrete damage traces from filamentation of Gauss-Bessel pulses," Opt. Lett. **31**, 80–82 (2006).
30. J. Song, X. Wang, X. Hu, Y. Dai, J. Qiu, Y. Cheng and Z. Xu, "Formation mechanism of self-organized voids in dielectrics induced by tightly focused femtosecond laser pulses," Appl. Phys. Lett. **92**, 092904 (2008).
31. S. Kanehira, J. Si, J. Qiu, K. Fujita, and K. Hirao, "Periodic Nanovoid Structures via Femtosecond Laser Irradiation," Nano Lett. **5**, 1591–1595 (2005).

1. Introduction

The nonlinear absorption of ultra short pulsed laser radiation in a transparent material offers a variety of different applications. It is a challenging task to control the energy deposition appropriately for tailoring the material modification suited to a specific process [1, 2]. With regard to in-volume machining, different modification mechanism are applied e.g. to write waveguides [3], to bond glass interfaces [4], to etch the laser modified regions with enhanced selectivity [5] or to locally weaken the material with tailored beams to enable a fast cutting process [6]. To increase process control and achieve a detailed understanding of the fundamental phenomena, down to a femtosecond timescale, in-situ observations of absorption and decay processes offer a deep insight into the laser material interaction.

The initial absorption process in the interplay between ultrashort pulsed laser radiation and

Optics EXPRESS

a transparent material is the deterministic generation of free electrons. These first seed electrons are produced via tunnel or multiphoton absorption, depending on the applied electric field strength. Due to the inverse bremsstrahlung the free electrons are accelerated in the electric field. Once they gained sufficient kinetic energy, a collision with bound electrons can excite new free charge carriers by means of impact ionization. As long as the electric field is strong enough to accelerate electrons, the latter process can amplify itself. Generally, this effect is denoted as avalanche ionization.

The geometrical shape of the absorbing volume is mainly determined by the intensity distribution of the incident laser radiation. Due to the typical peak power on a megawatt-scale of ultra short laser pulses, the propagation characteristic in matter can be altered significantly compared to vacuum. The main causes are the Kerr-Effect and the interaction of the pulse with ionized material. The most prominent result of these combined effects is the occurrence of filamentation. According to the strict physical definition this refers to a longitudinal extended zone where a part of the beam can propagate with a non-diffracting behavior due to an equilibrium state of Kerr lens self-focusing and plasma defocusing [7].

Subsequent to the absorption process a modification in the material starts to evolve due to a variety of decay mechanisms. Typically, the electron phonon interaction leads to a transfer of energy from the electron to the lattice subsystem. In consequence, different defects emerge. In fused silica the decay involves a relaxation of the electrons into self-trapped excitons followed by the formation of defects such as nonbridging oxygen-hole centers (NBOHC) and oxygen vacancies (E') [8]. These defects can further recombine into peroxy linkages (POL), peroxy radicals (POR) in combination with silicon-oxygen-deficiency centers (SiODC(II)) or SiODC(I) and interstitial oxygen (O_i) [9,10]. In mixed glasses, the decay mechanism incorporates a plenty of additional and mostly unknown defects [11]. On a macroscopic scale, these irregularities in the glass matrix result in a change of transmission which can be identified as color centers. Some of these point defects can be cured by annealing the material at a few hundred-degree Celsius [11]. Another aspect of the modified chemical linkage is a change in density and the refractive index, respectively. Besides the direct electronic processes, the extreme thermo-mechanical load in the laser-affected volume can change the material significantly. This comprises melting and resolidification [12], extreme mechanical stress, shockwaves and micro explosions [13].

Several in-situ investigations of these processes have been realized with pump-probe methods. For example Mao et. al. applied this technique to examine the transverse absorption, the electron-density and the temporal relaxation channels in fused silica glass under femtosecond irradiation [8]. The electron collision time and the plasma lifetime in fused silica were measured by Sun et. al. with shadowgraph imaging and an interferometric pump probe technique [14].

Pump probe imaging has also been used to study the material modification with nanosecond pulses [15], to observe ablation mechanisms in reflection and transmission [16] or to visualize the transient shock waves inside the material [17]. However, the geometrical extend of the transverse absorption was mainly imaged for sub picosecond pulses [18–20] in addition to a few intra-pulse studies [21].

Hence, there are still open questions on the geometrical and temporal evolution of the nonlinear absorption. Especially, the visualization of different absorption regimes, the intrapulse evolution of the electron density and incubation effects at different laser parameters would benefit from additional experimental data to analyze these phenomena. Therefore these questions are the content of the present paper.

In the first section we start with a description of our pump-probe setup. Subsequently, the absorption of a single ultra short laser pulse in the bulk material is investigated and the formation of a permanent modification is presented. To distinguish between filamentation and moving breakdown effects, we analyze different pulse and focusing conditions. The final section deals with incubation effects of multiple pulse processing, resulting in a self-organized modulation of

Optics EXPRESS

the longitudinal absorption.

2. Experimental setup

To investigate the spatial and temporal evolution of the electron density inside the material, we built up the pump probe setup, shown in Fig. 2. We use a Coherent® Libra® laser source with 2 mJ pulse energy and 100 fs pulse duration (FWHM) at a wavelength of 800 nm. The emitted pulsed laser radiation has a Gaussian beam profile and is split into a pump and a probe beamline. The probe pulse can be temporally adjusted with respect to the pump pulse via a delay line (100 nm minimum step size, 200 nm repeatability).

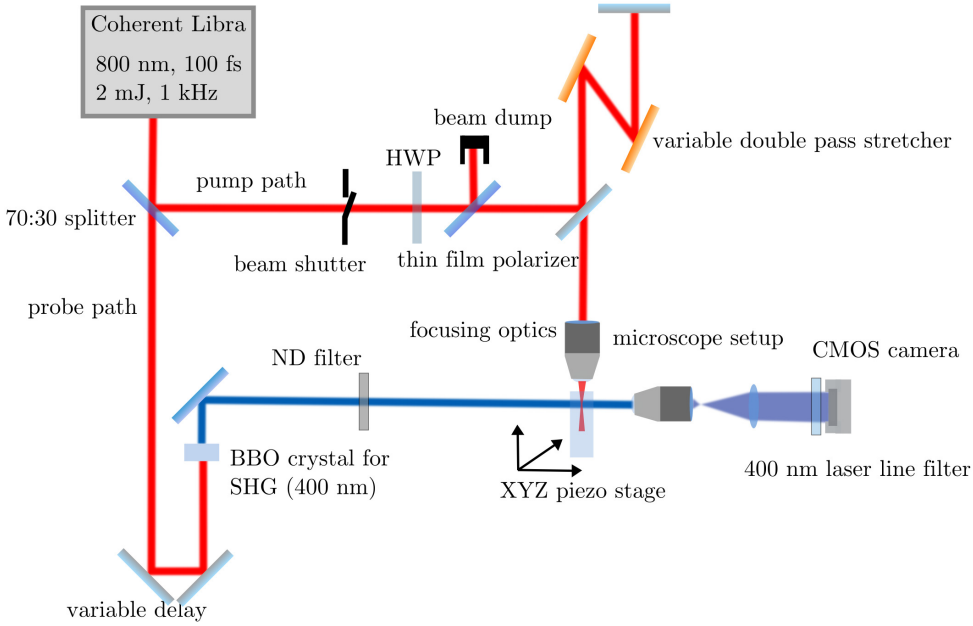

Fig. 1. Experimental pump-probe setup for the observation of the spatial and temporal absorption dynamics during ultra short pulse laser processing of transparent materials. The nonlinear absorption is measured perpendicular to the propagation direction of the machining beam with intra-pulse resolution due to an external stretcher in the pump beamline.

At the workpiece the frequency doubled and expanded probe pulse illuminates the glass sample perpendicular to the pump beam. To observe changes of the transmission inside the material with a sub 10 μm resolution, we use transmitted light microscopy (comprising either a 20x Mitutoyo® long WD or a 10x Olympus® objective combined with a 150 mm tube lens). A 400 nm laser line filter is integrated in front of the camera (IDS uEye® ML) to block scattered light from the perpendicular processing pump pulse and most of the plasma luminescence.

In the pump beamline, a half-wave plate and a thin-film polarizer are used to control the pulse energy. To independently change the pulse duration of the pump and the probe beam a double pass grating stretcher is integrated (two gold-coated gratings with 1500 l/mm). This enables the analysis of intra-pulse dynamics for pulse durations up to 5 ps with a temporal resolution determined by the probe pulse duration of 100 fs . The pump pulse-to-pulse stability of more than 99.8 percent enables an excellent reproducible imaging.

Finally, the linear polarized Gaussian pump beam is focused approximately 200 μm below the surface of the glass sample. In the following experiments all samples are 700 μm thick alkali-aluminum-silica glass (unhardened Corning Gorilla glass) with polished glass edges. We

Optics EXPRESS

restrict our experiments to unhardened glass to avoid any influence of the ion exchanged region on the propagation and the absorption of the laser radiation.

To generate shadowgraph images I_s single shot experiments are performed for different delays and laser parameters, each on a pristine sample position. Additional background images I_0 are recorded for all experiments. With this data the optical depth τ is calculated for each pixel using

$$\tau = \ln\left(\frac{I_0}{I_s}\right) = \int_0^l \kappa(l)\mathrm{d}l. \tag{1}$$

This calculated images allow to distinguish material which shows a significant nonlinear absorption of the pump pulse. Precisely, the optical depth represents an integral over all local extinction coefficients κ along one line l according to the Lambert-Beer law. Therefore an increased value of τ is observed when effects like absorption due to free electrons, transient states, defects or scattering losses reduce the local transmission of the probe pulse. In the following parts, we will name this pronounced area absorption zone.

3. Single pulse absorption

To analyze the absorption and formation dynamics of a modification, we operated our pump-probe setup at a pump pulse duration of 5 ps, a pulse energy of 30 μJ and a 6 mm raw beam diameter. The focal position was set approximately 200 μm below the glass surface using an Olympus® microscope objective (10 mm focal length, NA 0.46). In Fig. 2(a) we present the calculated images of the optical depth for different delays during the pump pulse absorption with intra-pulse resolution. Additionally, the corresponding isophotes are sketched around the estimated focal position. Figure 2(b) shows the decay of the optical depth, the formation of shock waves and an ex-situ microscope image of the permanent modification.

Within a time interval of 8 ps the electron density builds up in the observed zone. The plotted isophotes illustrate, that the absorption zone starts in the geometrical focus and expands in direction of the incoming laser pulse. This process can be ascribed to the moving breakdown effect [22]. During the leading pulse edge for pulse durations on a picosecond scale, the intensity depended threshold for nonlinear absorption moves in direction of the surface. Additionally the absorption zone becomes asymmetric due to the generation of free electrons and subsequent absorption. The average longitudinal growth speed was measured to approximately 20.7×10^6 m/s.

At a delay of 8 ps no change in the optical depth can be observed over a few picoseconds. We denote this maximized absorption zone as the first steady state. According to Fig. 2(b) a significant decay can be seen after 25 ps. It should be emphasized once again, that the experiment depicts the optical depth in the absorption zone. Therefore, the images include absorption due to free electrons, transient states or defects as well as scattering losses. We suppose that especially a few picoseconds after the first steady state, the absorption part from free electrons decreases and other afore mentioned effects start to dominate. Thus, the low transmission at the focal position after 25 ps is expected not to be based on free electrons.

We expect that the electronic recombination is the fastest relaxation channel. For example, Sun et. al. measured the plasma lifetime in fused silica to 170 fs [14]. Due to this fact, we assume that the fast signal decay in the moving breakdown region is an upper limit for the electron lifetime and all slower processes involve additional relaxation channels.

To observe contours of phase objects the following images at delays from 500 ps to 6.67 ns are recorded with a slightly defocused imaging setup to enhance the contrast of the phase-only objects. It has to be mentioned, that the defocusing does not change the appearance of the central absorption region in our experiments significantly. At 2.6 ns a symmetric structure can be observed which propagates cylindrically in transverse direction. The propagation speed is

Optics EXPRESS

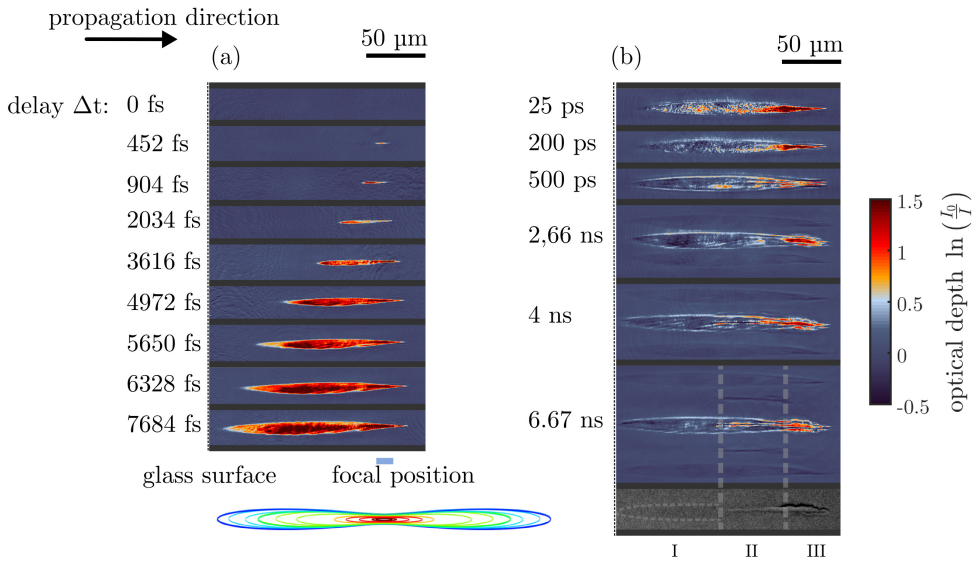

Fig. 2. Temporal evolution of the measured optical depth for a single pulse with 30 μJ pulse energy and 5 ps pulse duration, focused with a 10 mm objective into the volume. Part (a) shows the build up during the absorption of the laser pulse. For the corresponding focusing conditions, the isophotes are plotted below the pump probe images. Part (b) shows the decay of the optical depth and the formation of a shock wave. These Images from 500 ps to 6.67 ns use a slightly defocused imaging setup to enhance the contrast on the phase-only objects. The last contrast-enhanced transmission microscope image illustrates the permanent modification.

estimated to 5700 m/s. We ascribe this formation to a pressure wave, which starts approximately 500 ps after the pulse is absorbed and propagates through the glass with sonic velocity. After the structure has detached from the focal region, the geometry starts to change and matches the permanent modification after a few nanoseconds. At the timescale of 4-6 ns a second shock wave propagates through the volume. The comparison of the permanent modification with the time-resolved images shows three essential aspects. First, the volume with distinct color-centers in the permanent modification corresponds to the fast decay of the moving breakdown region I. Second, the bright region II of a strong, permanent phase change i.e. change in the refractive index, coincides with the second shock wave after 4-6 ns . Third, the dark, scattering focal structure III starts to evolve after 500 ps and presumably results from the first shock wave.

To study nonlinear absorption effects, we applied a pump pulse duration of 100 fs to generate higher intensities at constant pulse energies and focusing conditions. In Fig. 3 the corresponding buildup characteristic of the optical depth is shown. The absorption zone starts directly beneath the surface and expands with approximately 2×10^8 m/s, the speed of light in this glass, towards the focal position. A change of the optical depth beyond the focal plane has not been observed. Furthermore, the distinct permanent modification is generated at the focal position only.

Although the buildup direction is reversed compared to the experiments with a pulse duration of 5 ps, it can be described with the moving breakdown theory for ultrashort pulses [22]. Due to the connection between pulse duration and spatial pulse extend, the applied 100 fs pulse is localized over a few ten micrometers in longitudinal direction. In consequence, new electrons originating from pristine material are generated in this confined region of high intensity only. Hence, the total absorption zone extends in propagation direction with the speed of light in the

Optics EXPRESS

corresponding medium.

In comparison to the absorption characteristic of a 5 ps pulse, several differences can be mentioned. Due to an increased intensity, the 100 fs pulse produces an extended absorption zone, whereby the absorption starts at lower fluences in the beam caustic. In this region energy is deposited in the material without being sufficiently high enough to generate a distinct permanent modification. In consequence, the effective pulse energy at the focus is lowered due to continuous absorption in the propagation path. The resulting modification is much smaller and less pronounced for a 100 fs pulse duration compared to a pulse duration of 5 ps. We presume that type and magnitude of a modification depends on the effectively deposited energy density. In conclusion, the short pulse duration causes a large absorption zone and a slight modification in the focal plane.

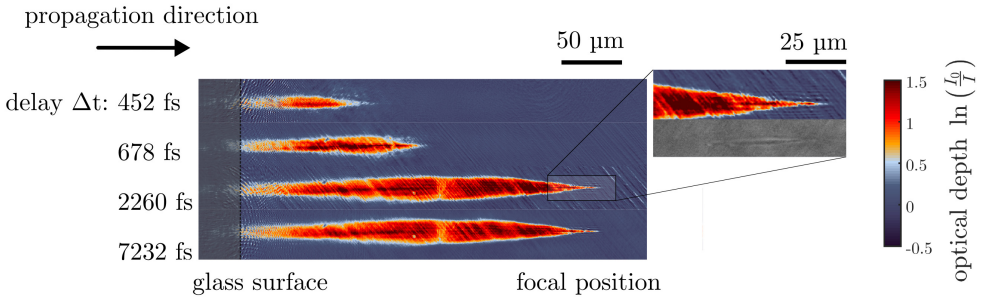

Fig. 3. Measured optical depth for a single pulse with 30 μJ pulse energy and a pulse duration of 100 fs, focused with a f = 10 mm microscope objective. The left part shows the growth of the absorption zone during the pulse propagation. On the right the permanent modification around the focus is magnified.

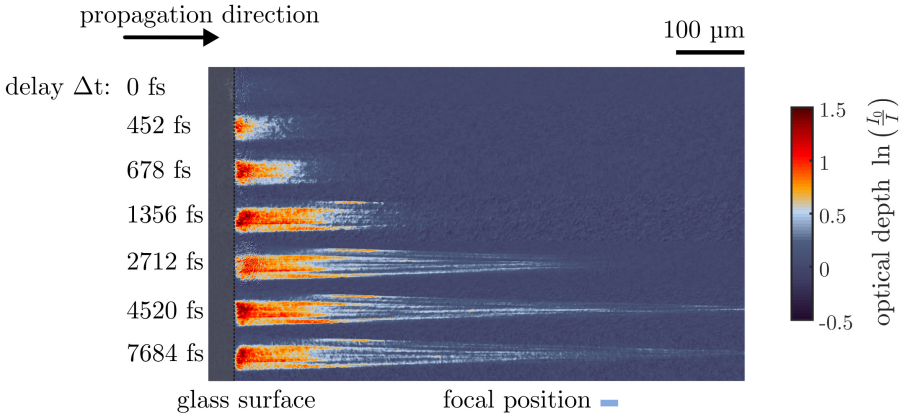

Fig. 4. Pump probe images for a single pulse with 50 μJ pulse energy and 100 fs pulse duration, focused by a lens with 50 mm focal length. Multiple filaments propagate through the medium with the speed of light .

To investigate a different propagation characteristic, we used a reduced effective NA of 0.05 at high intensities. The resulting temporal evolution for a single pulse with 50 μJ pulse energy and 100 fs pulse duration, focused by a lens with a focal length of 50 mm and a processing depth of approximately 500 μm, is shown in Fig. 4. The absorption starts directly at the surface and propagates through the medium with the speed of light. In this case many single filaments are

Optics EXPRESS

observed. All filaments converge behind the geometrical focus. These images indicate that a single filament starts in a point of sufficient intensity and propagates linearly through the medium while maintaining the wave vector of its starting position in the initial wavefront. These filaments can be observed even several Rayleigh lengths behind the focal position. A permanent modification of the sample after a single pulse has not been observed by transmitted light microscopy.

Scaling the pulse energy does not primarily influence the electron density in a single filament. In Fig. 5 the absorption zones for different pulse energies are shown. The peak power ranges from 50 MW for 5 μJ to 500 MW for 50 μJ. Each image corresponds to the first steady state, at a delay of approximately 8 ps. An increased pulse energy is distributed in additional filaments and does not substantially increase the optical depth of an individual filament. This characteristic is in accordance with observations of other groups [7]. Additionally, the increased intensity at higher pulse energies leads to a shift of the filament starting position towards the beam entrance surface.

To account for the influence of the Kerr effect, we estimate the self-focusing threshold power $P_{crit} = \alpha(\lambda^2/(4\pi n_0 n_2))$ [23]. Here λ is the wavelength, n_0, n_2 are the linear and nonlinear refractive index, respectively. We use $n_0 = 1.5$ and assume $n_2 = 3.4 \times 10^{-16}\text{cm}^2/\text{W}$ as similar to alkaline glasses [24, 25]. The constant α for a Gaussian beam is approximated with $\alpha = 1.9$ [23]. Based on these assumptions the value of P_{crit} corresponds to 1.9 MW. It should be mentioned that the nonlinear refractive index for linear polarization, as used in our experiments, is increased by a factor of 1.5 compared to circular polarization in an isotropic material [26]. This implicates a lower self-focusing threshold for linear polarized radiation.

For both pulse durations (100 fs and 5 ps), focused by an objective with 10 mm focal length, the peak powers of 300 MW and 6 MW exceed the self-focusing threshold by at least two orders of magnitude. However, for these tight focusing conditions, we could not observe a longitudinal increased optical depth beyond the focal position in contrast to loose focusing conditions with a focal length of 50 mm and a pulse duration of 100 fs.

The observed significant differences of filament generation in dependence of the focusing conditions correspond to observations of other groups in fused silica [27, 28]. Their experimental investigations of the generated super continuum were carried out for different focusing conditions to distinguish between optical breakdown and filamentation regime. These experiments showed a suppressed white-light-generation under tight focusing which can be interpreted as suppressed extended filaments.

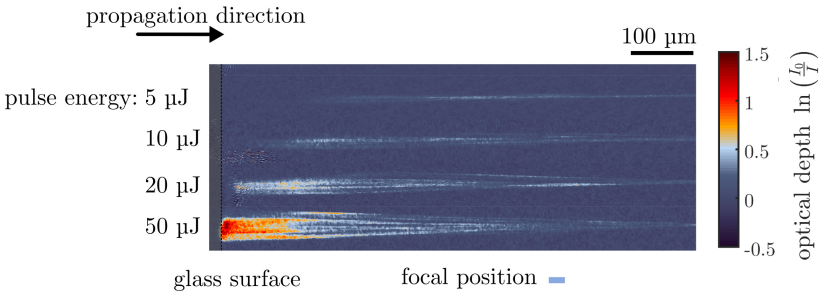

Fig. 5. Images of the optical depth in the first steady state, at a 8 ps delay for different pulse energies. The pulse with a pulse duration of 100 fs was focused by a lens with 50 mm focal length. The images show a spatial shift of the filament starting position towards the surface and the formation of multiple filaments with an increased pulse energy.

Optics EXPRESS

4. Multiple pulse absorption

In the following experiments, we investigated incubation effects by deposition of multiple pulses at a fixed position. Due to the repetition rate of 1 Hz heat accumulation can be neglected. Under these conditions, we observe a self-organization effect of the optical depth presumably resulting from a self-organized electron density as illustrated in Fig. 6(a). The image series shows the absorption zones in the first steady state, at a delay of 8 ps. The pulse energy in these experiments was chosen to 10 μJ at a pulse duration of 5 ps. The beam was focused approximately 200 μm below the glass surface using the aforementioned microscope objective with a focal length of 10 mm. From the left to the right hand side, the number of pulses deposited at the same position are increased from 1 to 20. Each image represents the absorption at a 8 ps delay after the last pulse.

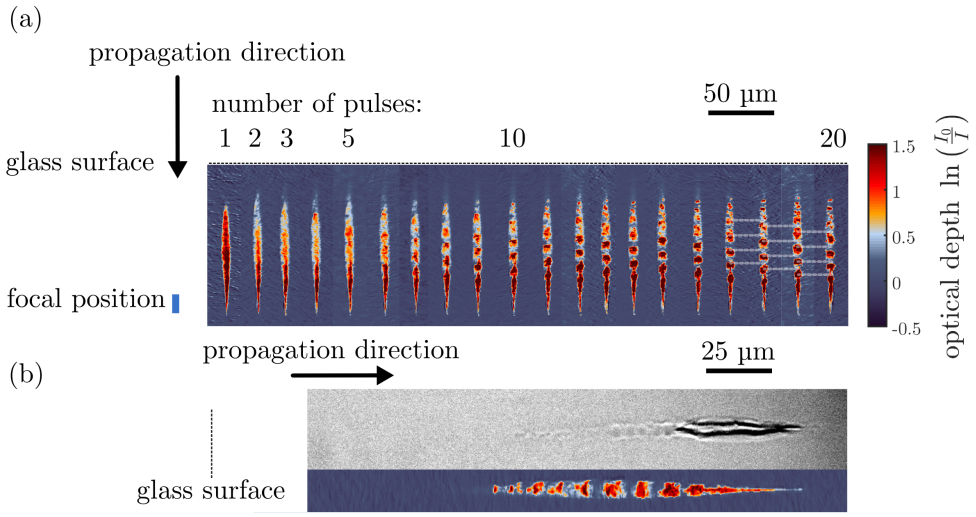

Fig. 6. Incubation effects by multiple pulse deposition at the same position. The pump probe images in (a) show the optical depth of the last pulse for 1 to 20 pulses per position. The repetition rate was 1 Hz with 10 μJ pulse energy in each pulse. The pulses with a pulse duration of 5 ps were focused with a f = 10 mm microscope objective. The images show the first steady state after approximately 8 ps. A self organizing structure develops after a few pulses. Part (b) shows a grayscale, ex-situ transmission microscope image after 30 pulses and the corresponding optical depth image.

This data indicate that the absorption of a second pulse is stronger localized at the focal position. With the third pulse a first hot spot is created at the low fluence end of the absorption zone. With each additional pulse the hot spots move towards the focal position and show an increasing optical depth, while additional spots are generated in the low fluence region. The resulting structure shows a reproducible uniformity with a spacing between the central hotspots of approximately 4-6 μm. A comparison of two consecutive pulses shows, that the hot spots are formed almost exactly in the gaps of the prior pulse. For the last four pulses this is visualized with dashed lines which trace the hot spots from one pulse to the next gap.

Moreover, the permanent modification after 30 pulses is shown in Fig. 6(b) with the corresponding pump-probe measurement. This image indicates that a superposition of all spherical hot spots leads to a slight permanent modification of the refractive index.

Longitudinal modulated modifications were observed in transparent materials from other groups, for example by using a Bessel beam [29]. The modulation period in these experiments was measured to 9 μm. Moreover, modulated structures with a period between approximately

Optics EXPRESS

1-10 μm were observed with Gaussian beams under tight focusing using a NA of 0.9 and a focal position several hundred micrometers beneath the surface [30, 31]. These effects were mainly ascribed to nonlinear propagation or aberration effects.

We assume that a modulation of the absorption, induced due to nonlinear propagation, should be visible in the single pulse experiment as a consequence of the changed spatial intensity distribution.

Such modulations are not observed in our single pulse experiments. In fact, several pulses are required to generate the modulation. This leads us to the conclusion that the dominant effect in our experiments is due to an incubation effect rather than a pure nonlinear propagation effect.

We propose the following explanation for our observations.

In regions with moderate electron density and sufficient fluence, long living defects are generated, which increase the local absorption. The increased absorption of the subsequent laser pulse induces the formation of local hot spots which shield the adjacent area. In consequence, the electron density remains moderate in the adjacent area, which promotes new defect generation.

However, the excessive electron density in the transient hot spots results in an increased temperature, which on the other hand is capable to cure local defects as aforementioned. Probably this effect quenches the defects in the current hot spots, so that the material shows no significant increased absorption in these regions afterwards.

In conclusion, this alternating process of defect generation and quenching of the induced hot spots by subsequent pulses leads to the longitudinal modulation.

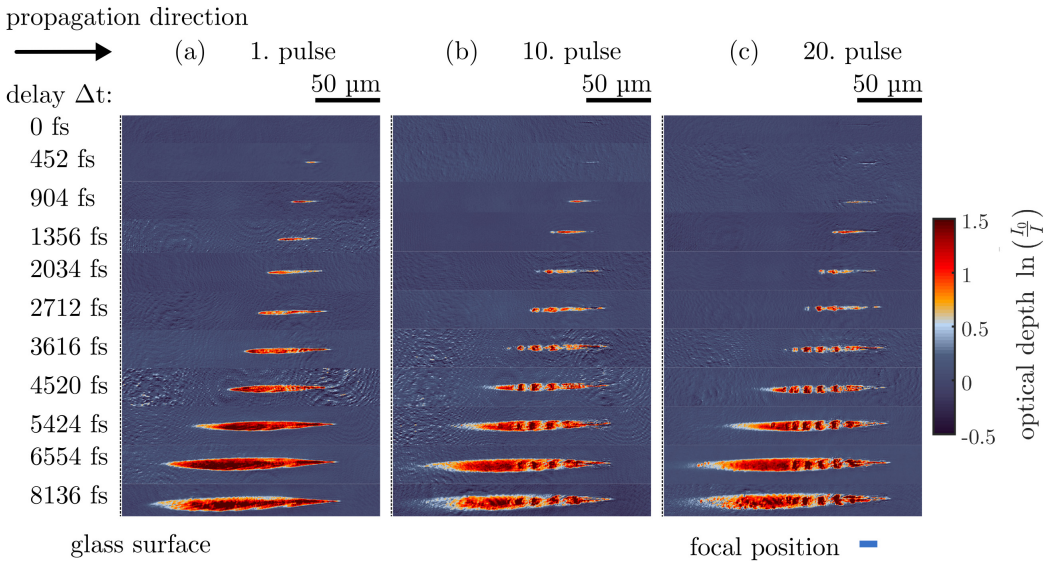

Fig. 7. Pump probe images of the measured optical depth during absorption for (a) the first, (b) the 10. and (c) the 20. pulse on the same position. The pulse energy is 30 μJ with 5 ps pulse duration at 1 Hz repetition rate using a f = 10 mm microscope objective. The self organizing hot spots are reproducible generated, considering that each time frame is produced on a different sample position.

For further insight, the temporal intra-pulse evolution of the first, the 10th and the 20th pulse is shown in Fig. 7 for a pulse energy of 30 μJ. Obviously, the hot spot structure is excellent reproducible due to the fact that each delay corresponds to an independent experiment generated on a different sample position. Furthermore, the images indicate, that a higher pulse energy does not

Optics EXPRESS

lead to a modulation in the extended absorption zone. The hot spots are generated close to the focus, while the absorption remains constant in the region of decreased fluence. However, the typically temporal moving breakdown characteristic is unaffected from the modulation. Hence, the hot spots emerge slowly within every single pulse absorption, always starting near the focal position.

5. Conclusion

In this paper, we presented in-situ pump-probe measurements of absorption phenomena in unhardened Corning Gorilla glass. The intra-pulse evolution of a single, tightly focused, 5 ps pulse was analyzed, as well as the decay of the optical depth and the formation of a permanent modification. We compared the moving breakdown characteristic during the absorption process between a pulse duration of 5 ps and 100 fs and discussed the differences in the permanent modification. We observed distinct longitudinal extended filaments beyond the focal position solely under loose focusing conditions and presented the transition from single to multiple filaments with increasing pulse energy.

Finally, we investigated incubation effects with negligible thermal accumulation of tightly focused 5 ps pulses. Our observations show a self-organizing effect of the absorption with excellent reproducibility. This effect manifests in a longitudinal modulation of the electron density with approximately 5 μm spacing, whereupon the absorption centers are erased with each following pulse but contribute to a permanent modification.

Funding

Federal Ministry of Education and Research (BMBF) (13N13309).